NEGATIVE RESULTS ON CONTROL OF CHAOTIC CIRCUITS

Zbigniew Galias*, Josef A. Nossek† and Maciej J. Ogorzałek*

*Department of Electrical Engineering, University of Mining and Metallurgy
al. Mickiewicza 30, 30-059 Kraków, Poland
†Institute of Network Theory and Circuit Design, Technical University Munich
Arcisstr. 21, D-80290 Munich, Germany

Abstract

In this paper we investigate the possibilities of applying the OGY control method to the three-cell CNN chaotic system. We address the problem, why it is very difficult or even impossible to achieve successful control in computer simulations and real experiments. The theorem, which can be useful for proving the existence of unstable periodic orbits is formulated. Using this theorem we prove the existence of the period-1 orbit. We calculate its Jacobian analytically and find the size of the neighbourhood, in which the linearisation of the system's behaviour in the vicinity of this periodic orbit is valid. We show this size to be very small. Finally we give several reasons why it is very difficult to implement this control method in real chaotic systems.

1 Introduction

In this paper we consider an autonomous three-cell CNN with the dynamics described by the following state equations:

$$\begin{aligned} \dot{x}^1 &= -x^1 + p_1 f(x^1) - s f(x^2) - s f(x^3) \\ \dot{x}^2 &= -x^2 - s f(x^1) + p_2 f(x^2) - r f(x^3) \\ \dot{x}^3 &= -x^3 - s f(x^1) + r f(x^2) + p_3 f(x^3), \end{aligned} \tag{1}$$

where $f(\cdot)$ is a saturation characteristic

$$f(x) = 0.5(|x+1| - |x-1|) \tag{2}$$

with the following parameter set: $p_1 = 1.25$, $p_2 = 1.1$, $p_3 = 1$, $s = 3.2$, $r = 4.4$. For this set of parameters a chaotic attractor has been observed [7].

The OGY control method [5] has been applied for stabilization of the period-1 orbit of the above system. In the case of a three-dimensional dynamical system this method can be used for the stabilization of any periodic orbit embedded within the chaotic attractor, if only some system parameter is available for the control. In the simplest case of single-point method the control parameter is modified only when the system trajectory intersects a chosen hyperplane. It is changed in such a way, that the next intersection of this hyperplane by the trajectory will fall onto the stable manifold of the periodic orbit.

2 Preliminaries

Let us divide the state space into 27 regions Ω_{ijk}, with $i, j, k \in \{-1, 0, +1\}$, defined by:

$$\Omega_{i,j,k} := \{\boldsymbol{x} = (x^1, x^2, x^3)^T : x^1 \in A_i, x^2 \in A_j, x^3 \in A_k\},$$

where $A_{-1} = (-\infty, -1)$, $A_0 = [-1, +1]$, $A_{+1} = (+1, \infty)$. In each of these regions the system (1) is linear, hence one can calculate the solution without numerical integration. Let us denote the planes being the boundaries of the Ω_{ijk} by $H_i^{\pm} := \{\boldsymbol{x} \in \mathbb{R}^3 : \boldsymbol{e}_i^T \boldsymbol{x} = \pm 1\}$. In the region Ω_{ijk} the system equation can be written as:

$$\dot{\boldsymbol{x}} = \boldsymbol{A}_{ijk}\boldsymbol{x} + \boldsymbol{v}_{ijk}.$$

If the matrix $\boldsymbol{A}_{ijk}$ is invertible then one can rewrite the above equation in the form: $\dot{\boldsymbol{x}} = \boldsymbol{A}_{ijk}(\boldsymbol{x} - \boldsymbol{P}_{ijk})$, where $\boldsymbol{P}_{ijk} = \boldsymbol{A}_{ijk}^{-1}\boldsymbol{v}_{ijk}$. Hence the solution can be calculated as

$$\boldsymbol{x}(t) = e^{\boldsymbol{A}_{ijk}t}(\boldsymbol{x}(0) - \boldsymbol{P}_{ijk}) + \boldsymbol{P}_{ijk}.$$

Unfortunately not all of the matrices $\boldsymbol{A}_{ijk}$ are invertible. For instance in the region Ω_{110} the linear part of the state equation is

$$\boldsymbol{A}_{110} = \begin{bmatrix} -1 & 0 & -s \\ 0 & -1 & -r \\ 0 & 0 & 0 \end{bmatrix},$$

which is a non-invertible matrix. Similar situation happens for all triples (i,j,k) such that $i,j \neq 0$ and $k = 0$. However in this case we can also find analytically the solution of the system. Namely if

$$\dot{\boldsymbol{x}} = \boldsymbol{A}\boldsymbol{x} + \boldsymbol{v} = \begin{bmatrix} -1 & 0 & a_{13} \\ 0 & -1 & a_{23} \\ 0 & 0 & 0 \end{bmatrix} \boldsymbol{x} + \begin{bmatrix} v_1 \\ v_2 \\ v_3 \end{bmatrix} \tag{3}$$

is the state equation, then the solution of the system is

$$\boldsymbol{x}(t) = \boldsymbol{b}_0 + \boldsymbol{B}_1\boldsymbol{x}(0) + \boldsymbol{b}_2 t + \boldsymbol{b}_3 e^{-t} + \boldsymbol{B}_4\boldsymbol{x}(0)e^{-t}, \tag{4}$$

where

$$\boldsymbol{b}_0 = \begin{bmatrix} v_1 - a_{13}v_3 \\ v_2 - a_{23}v_3 \\ 0 \end{bmatrix}, \boldsymbol{B}_1 = \begin{bmatrix} 0 & 0 & a_{13} \\ 0 & 0 & a_{23} \\ 0 & 0 & 1 \end{bmatrix}, \boldsymbol{b}_2 = \begin{bmatrix} a_{13}v_3 \\ a_{23}v_3 \\ v_3 \end{bmatrix}, \boldsymbol{b}_3 = -\boldsymbol{b}_0, \boldsymbol{B}_4 = \begin{bmatrix} 1 & 0 & -a_{13} \\ 0 & 1 & -a_{23} \\ 0 & 0 & 0 \end{bmatrix}.$$

3 The period-1 orbit

During computer simulations we have found a periodic orbit, which intersects the boundaries of the regions $\Omega_{i,j,k}$ six times and visits five of these regions. Let us denote by $\boldsymbol{x}_1, \boldsymbol{x}_2, \ldots, \boldsymbol{x}_6$ the succesive intersection points of the periodic orbit with the boundaries of the regions $\Omega_{i,j,k}$. Because we know the solutions of the system in the linear regions we can write down the analytical conditions for the fixed point:

$$\begin{aligned} \boldsymbol{x}_{i+1} &= e^{\boldsymbol{A}_i t_i}(\boldsymbol{x}_i - \boldsymbol{P}_i) + \boldsymbol{P}_i =: f_i(\boldsymbol{x}_i, t_i) \;\; for \;\; i = 1, \ldots, 4 \\ \boldsymbol{x}_6 &= \boldsymbol{b}_0 + \boldsymbol{B}_1\boldsymbol{x}_5 + \boldsymbol{b}_2 t_5 + \boldsymbol{b}_3 e^{-t_5} + \boldsymbol{B}_4\boldsymbol{x}_5 e^{-t_5} =: f_5(\boldsymbol{x}_5, t_5) \\ \boldsymbol{x}_1 &= e^{\boldsymbol{A}_6 t_6}(\boldsymbol{x}_6 - \boldsymbol{P}_6) + \boldsymbol{P}_6 =: f_6(\boldsymbol{x}_6, t_6) \end{aligned} \tag{5}$$

$$\boldsymbol{x}_1 \in H_1^+, \boldsymbol{x}_2 \in H_1^+, \boldsymbol{x}_3 \in H_3^-, \boldsymbol{x}_4 \in H_2^+, \boldsymbol{x}_5 \in H_3^-, \boldsymbol{x}_6 \in H_2^- \tag{6}$$

$$f_p(x_p, t)^j \in \bigcup_{ijk} int\Omega_{ijk} \;\; for\ every\ t \in (0, t_p), p \in \{1, \ldots, 6\}. \tag{7}$$

The conditions (6) and (7) are called the boundary conditions and the open conditions respectively. The boundary conditions state that the points $\boldsymbol{x}_i$ belong to the boundaries of the linear regions while the open conditions state that no other points on the periodic orbit lie on the boundaries of the linear regions. It is possible to find a solution of the system (5,6,7) numerically. We are not sure however, whether the solution found is not a computer artifact. In order to prove the existence of the period-1 orbit we will use the following theorem:

Theorem 1. *Let $D \subset Q$ be the set possessing the fixed point property*[1] *and f be a continuous function $f : D \longrightarrow Q$. Let A_1, A_2 be the closed disjoint subsets of D such that*

$$f(A_1) \cap D \subset A_2 \tag{8}$$
$$f(A_2) \cap D \subset A_1 \tag{9}$$
$$f(D \setminus (A_1 \cup A_2)) \subset D \tag{10}$$

and there exists a retraction[2] *g of Q into D such that $g(f(A_2)) \subset A_1$ and $g(f(A_1)) \subset A_2$. Then the function f has a fixed point $x_F \in B := D \setminus (A_1 \cup A_2)$.*

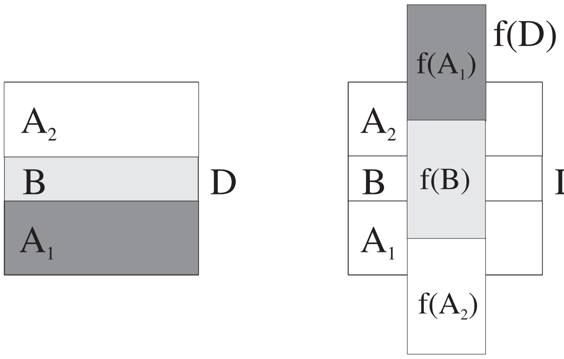

Figure 1: Sets D, A_1, A_2, B and their images under map f.

Proof. Let $h := g \circ f$. Because $h(D) \subset D$ and D has the fixed point property, then there exists a fixed point x_F of function h. Now we prove that $x_F \in B$.
1. If $x_F \in A_1$ then $f(x_F) \in f(A_1)$ and from the properties of retraction g it follows that $g(f(x_F)) \in A_2$. Hence $x_F \neq h(x_F)$ because $A_1 \cap A_2 = \emptyset$.
2. Similarly we obtain a contradiction if we assume that $x_F \in A_2$. Thus $x_F \in B = D \setminus (A_1 \cup A_2)$. From (10) it follows that $f(x_F) \in D$. As g is a retraction then $g(x) = x$ for $x \in D$. Hence $g(f(x_F)) = f(x_F)$. Thus function f possesses a fixed point $x_F \in B$. □

Remark 1. *From the Brouwer's fixed point theorem it follows that every set homeomorphic to $I^2 = [0, 1]^2$ possesses the fixed point property.*

Remark 2. *Let $D = \overline{EFGH}$ be a parallelogram, such that $f(D)$ is enclosed in the stripe defined by one pair of parallel sides of D (for example $\overline{EH}$ and $\overline{FG}$). Let A_1 and A_2 be subsets of D such that $\overline{EF} \subset A_1$, $\overline{GH} \subset A_2$ and conditions (8)..(10) are fulfilled. Then there exists a retraction g such that $g(f(A_2)) \subset A_1$ and $g(f(A_1)) \subset A_2$.*

Proof: As a retraction we can choose projection onto sides $\overline{GH}$ and $\overline{EF}$ in the direction $\overline{EH}$.

The above theorem can be useful in computer-aided proofs of existence of fixed points of two– or higher–dimensional maps, when the fixed point possesses one unstable eigenvalue with negative sign. Because all assumptions about f are inclusions of images of some sets one does not have to ensure infinite precision in calculations to check these assumptions.

In order to prove the existence of the period-1 orbit we have considered the Poincaré map $P = P_\Sigma$, with the surface of section $\Sigma = H_1^+$. We have found a parallelogram D with two subsets A_1, A_2 satisfying assumptions of Theorem 1 (compare Fig. 2(a)). Conditions (8)..(10) have been checked by computer. Having exact solutions in the linear regions, we were able to keep the computation error small.

[1] We say that a set has the *fixed point property* if for every continuous map from this set into itself there exists a fixed point of this map.

[2] A continuous function $g : Q \longrightarrow D \subset Q$ is called a *retraction* if $g(x) = x$ for every $x \in D$.

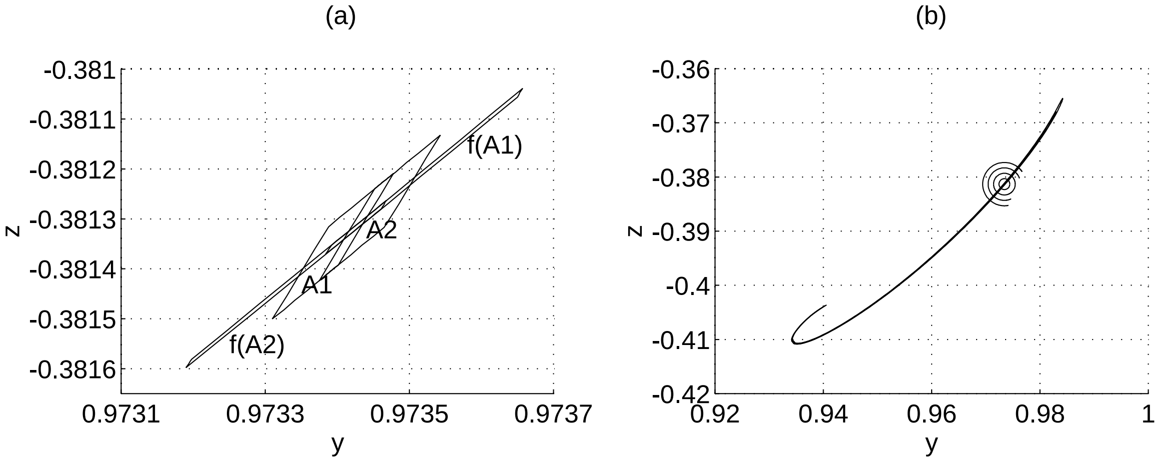

Figure 2: (a) Sets A_1 and A_2 and their images under Poincaré map associated with the 3-cell CNN system. (b) Images of circles centered at fixed point under Poincaré map.

Once we are sure that the fixed point exists, we can find its approximate position:

$$\boldsymbol{x}_1 = (1, 0.973426, -0.381316)^T \tag{11}$$

4 Computation of the Jacobian

The next step in the control procedure is calculation of the Jacobian of the chosen periodic orbit. We will calculate the Jacobian of the fixed point on the Poincaré map associated with the periodic orbit considered. The period-1 orbit intersects the boundaries $H_i^{\pm}$ six times. In such case it is natural to decompose the Poincaré map P_Σ into six generalized Poincaré maps, compute their Jacobians and then multiply these Jacobians in order to obtain the Jacobian of the full Poincaré map. First we derive the formula for the Jacobian in the case when the matrix $\boldsymbol{A}_{ijk}$ is invertible (the method is similar to the one used in [4]).

Lemma 1. *If the trajectory based at $\boldsymbol{x}_0$ reaches $\boldsymbol{y}_0$ after time t_0, $\Sigma_1 = \{\boldsymbol{x} : e_j^T \boldsymbol{x} = e_j^T \boldsymbol{x}_0\}$, $\Sigma_2 = \{\boldsymbol{x} : e_i^T \boldsymbol{x} = e_i^T \boldsymbol{y}_0\}$ are the hyperplanes transversal to the trajectory and the solution of the system is given by $\boldsymbol{x}(t) = e^{\boldsymbol{A}t}(\boldsymbol{x}(0) - \boldsymbol{P}) + \boldsymbol{P}$ then the Jacobian of the generalized Poincaré map $P_{\Sigma_1\Sigma_2}$ at $\boldsymbol{x}_0$ is the ij-th minor of the matrix*

$$\left[\boldsymbol{I} - \frac{\boldsymbol{A}(\boldsymbol{y}_0 - \boldsymbol{P})e_i^T}{e_i^T \boldsymbol{A}(\boldsymbol{y}_0 - \boldsymbol{P})}\right] e^{\boldsymbol{A}t_0}. \tag{12}$$

Proof. Let us define $\boldsymbol{F}(\boldsymbol{x}, t) = e_i^T(e^{\boldsymbol{A}t}(\boldsymbol{x} - \boldsymbol{P}) + \boldsymbol{P}) - e_i^T \boldsymbol{y}_0$. It is clear that

$$\boldsymbol{F}(\boldsymbol{x}_0, t_0) = e_i^T(e^{\boldsymbol{A}t_0}(\boldsymbol{x}_0 - \boldsymbol{P}) + \boldsymbol{P}) - e_i^T \boldsymbol{y}_0 = e_i^T \boldsymbol{y}_0 - e_i^T \boldsymbol{y}_0 = 0, \tag{13}$$

$$\frac{\partial \boldsymbol{F}}{\partial t}(\boldsymbol{x}_0, t_0) = e_i^T \boldsymbol{A} e^{\boldsymbol{A}t_0}(\boldsymbol{x}_0 - \boldsymbol{P}) = e_i^T \boldsymbol{A}(\boldsymbol{y}_0 - \boldsymbol{P}) \neq 0. \tag{14}$$

Hence there exists a neighbourhood U of $\boldsymbol{x}_0$ and a function $t : U \ni \boldsymbol{x} \longrightarrow t(\boldsymbol{x}) \in \mathbb{R}$ such that for every $\boldsymbol{x} \in U$ $\boldsymbol{F}(\boldsymbol{x}, t(\boldsymbol{x})) = 0$ and $t(\boldsymbol{x}_0) = t_0$.

$$\boldsymbol{D}t(\boldsymbol{x}_0) = -\left[\frac{\partial \boldsymbol{F}}{\partial t}(\boldsymbol{x}_0, t_0)\right]^{-1} \frac{\partial \boldsymbol{F}}{\partial \boldsymbol{x}}(\boldsymbol{x}_0, t_0) = -[e_i^T \boldsymbol{A}(\boldsymbol{y}_0 - \boldsymbol{P})]^{-1} e_i^T e^{\boldsymbol{A}t_0}. \tag{15}$$

Let us define a map $f(\boldsymbol{x}) = e^{\boldsymbol{A}t(\boldsymbol{x})}(\boldsymbol{x} - \boldsymbol{P}) + \boldsymbol{P}$. In order to compute the derivative of f let us decompose the map f in the following way: $f(\boldsymbol{x}) = (h \circ g)(\boldsymbol{x})$, where $g(\boldsymbol{x}) = (\boldsymbol{x}, t(\boldsymbol{x}))$, $h(\boldsymbol{x}, \boldsymbol{y}) = e^{A\boldsymbol{y}}(\boldsymbol{x} - \boldsymbol{P}) + \boldsymbol{P}$,

$\boldsymbol{D}g(\boldsymbol{x}) = (\boldsymbol{I}, \boldsymbol{D}t(\boldsymbol{x}))^T$ and $\boldsymbol{D}h(\boldsymbol{x},\boldsymbol{y}) = (e^{\boldsymbol{A}\boldsymbol{y}}, \boldsymbol{A}e^{\boldsymbol{A}\boldsymbol{y}}(\boldsymbol{x}-\boldsymbol{P}))$.

$$\begin{aligned}
\boldsymbol{D}f(\boldsymbol{x}_0) &= \boldsymbol{D}h(\boldsymbol{x}_0, t(\boldsymbol{x}_0)) \cdot \boldsymbol{D}g(\boldsymbol{x}_0) = (e^{\boldsymbol{A}t(\boldsymbol{x}_0)}, \boldsymbol{A}e^{\boldsymbol{A}t(\boldsymbol{x}_0)}(\boldsymbol{x}_0 - \boldsymbol{P})) \cdot (\boldsymbol{I}, \boldsymbol{D}t(\boldsymbol{x}_0))^T \\
&= e^{\boldsymbol{A}t(\boldsymbol{x}_0)}\boldsymbol{I} + \boldsymbol{A}e^{\boldsymbol{A}t(\boldsymbol{x}_0)}(\boldsymbol{x}_0 - \boldsymbol{P})\boldsymbol{D}t(\boldsymbol{x}_0) \\
&= e^{\boldsymbol{A}t_0} - \boldsymbol{A}(\boldsymbol{y}_0 - \boldsymbol{P})[e_i^T\boldsymbol{A}(\boldsymbol{y}_0 - \boldsymbol{P})]^{-1}e_i^T e^{\boldsymbol{A}t_0} \\
&= \left[\boldsymbol{I} - \frac{\boldsymbol{A}(\boldsymbol{y}_0 - \boldsymbol{P})e_i^T}{e_i^T\boldsymbol{A}(\boldsymbol{y}_0 - \boldsymbol{P})}\right] e^{\boldsymbol{A}t_0}.
\end{aligned}$$

$\boldsymbol{D}f(\boldsymbol{x}_0)$ is the Jacobian of the three-dimensional function $f = (f^1, f^2, f^3)$ of three variables x^1, x^2, x^3. From the construction f it follows that $f^i \equiv 0$, which correspond to zero i-th row of the matrix $\boldsymbol{D}f(\boldsymbol{x}_0)$. Because the map f is defined on the plane $\{\boldsymbol{x} : \boldsymbol{e}_j^T\boldsymbol{x} = const\}$ then it is clear that we must remove the i-th row and the j-th column from $\boldsymbol{D}f(\boldsymbol{x}_0)$ in order to obtain the Jacobian of the generalized Poincaré map. □

For the case when the matrix $\boldsymbol{A}$ is non-invertible and the solution is described by equation (4) the Jacobian is the ij-th minor of the matrix

$$\boldsymbol{D}f(\boldsymbol{x}_0) = \left[\boldsymbol{I} - \frac{(\boldsymbol{b}_2 - \boldsymbol{b}_3e^{-t_0} - \boldsymbol{B}_4\boldsymbol{x}_0e^{-t_0})e_i^T}{e_i^T(\boldsymbol{b}_2 - \boldsymbol{b}_3e^{-t_0} - \boldsymbol{B}_4\boldsymbol{x}_0e^{-t_0})}\right](\boldsymbol{B}_1 + \boldsymbol{B}_4e^{-t_0}). \tag{16}$$

The proof is very similar to the proof in the previous case.

Now we can compute the Jacobian of the full Poincaré map as

$$\boldsymbol{J} = \boldsymbol{D}f_6(\boldsymbol{x}_6)_{12} \cdot \boldsymbol{D}f_5(\boldsymbol{x}_5)_{23} \cdot \boldsymbol{D}f_4(\boldsymbol{x}_4)_{32} \cdot \boldsymbol{D}f_3(\boldsymbol{x}_3)_{23} \cdot \boldsymbol{D}f_2(\boldsymbol{x}_2)_{31} \cdot \boldsymbol{D}f_1(\boldsymbol{x}_1)_{11},$$

where $\boldsymbol{D}f(\boldsymbol{x})_{ij}$ denotes the ij-th minor of matrix $\boldsymbol{D}f(\boldsymbol{x})$.

One can also first multiply Jacobians $\boldsymbol{D}f_j$ in the same order and then remove the first row and first column from the result to obtain the Jacobian of the full Poincaré map.

Using the approximation of the fixed point (11) we have found the Jacobian of the Poincaré map to be

$$\boldsymbol{J} = \begin{bmatrix} -5.7767 & 2.3839 \\ -6.7152 & 2.7238 \end{bmatrix}. \tag{17}$$

Its eigenvalues are $\lambda_s = -0.0924$, $\lambda_u = -2.9604$.

5 Size of neighbourhood with “good” linear approximation

In the previous sections the approximate position of the periodic orbit and its Jacobian have been found (without numerical integration, with very good accuracy). The calculated values agree quite well with the values computed from the data series obtained using numerical integration.

To study the effect of noise we have added the term $\varepsilon\delta_n$ to the time series, where ε is a small parameter specifying the level of noise and δ_n is a three-dimensional random variable $\delta_n \in [-1,1]^3$.

For $\varepsilon = 0.0005$ the control method worked properly, but for $\varepsilon = 0.001$ we were not able to stabilize the chosen periodic orbit. Similar effect has been obtained for different integration time steps, when we have used Runge-Kutta integration method instead of exact solutions presented in the first part of the paper. For the time step $\tau = 0.005$ the control method worked well and for $\tau = 0.01$ the control was unsuccessful. Greater time step is equivalent to the higher level of noise in computing Poincaré map. In Fig. 2(b) one can see circles centered at the fixed point and their images under Poincaré map. Only these points from the circles are painted in black, whose images under Poincaré map return into the small neighbourhood of the fixed point. The existence of a continuous Poincaré map is ensured only locally. This corresponds to the broken circles in Fig. 2(b).

We have observed that trajectories based at certain points very close to the fixed point intersect the hyperplane H_1^- and enter the second part of the attractor. In order to find such points it is enough to solve the condition:

$$\boldsymbol{e}_1^T e^{\boldsymbol{A}t_0}\boldsymbol{x}_0 = -1 \tag{18}$$

simultaneously with the open condition:

$$\boldsymbol{e}_1^T e^{\boldsymbol{A}t}\boldsymbol{x}_0 \in \Omega_{000} \ \ \forall t \in [0, t_0] \tag{19}$$

where $\boldsymbol{x}_0 = (1, y_0, z_0)^T$. We have found a pair $(y_0, z_0) = (0.976024, -0.382350)$ satisfying (18,19). It lies very close to the fixed point, its distance from the fixed point is $d = 0.0028$. The existence of a point satisfying (18,19) is an explanation for the broken circles in Fig. 2(b).

Now it is clear that there are two main reasons for which the linear approximation is not good enough. The first reason is that the continuous Poincaré map could be defined only in a small neighbourhood of the fixed point. Such a neighbourhood could be too small to ensure a successful control of the periodic orbit. If we are unable to keep the trajectory inside this small neighbourhood all the time the successful control cannot be obtained any more. In our case the circle with radius 0.003 is not completely enclosed inside the domain of the continuous Poincaré map.

The second reason could be the existence of nonlinear terms (compare folding of image of the greatest circle with radius 0.004 in Fig. 2(b)). In an ideal experiment we can modify the original OGY method and include higher-order terms in approximation of the system's behaviour around the periodic orbit. In experimental situation however, such a modification is not helpful. Due to the noise it is difficult to find good approximations of linear terms. It is even more difficult to compute nonlinear ones.

6 Conclusions

The OGY method works well in theory and very accurate computer simulations. In real experiments however it is very hard to implement it successfully.

In theory if the linearisation is not good or the Poincaré map is defined only in a very small neighbourhood of the fixed point we can decrease the neighbourhood size (one of the method's properties is that the control can be achieved with arbitrarily small parameter changes). In practice we cannot decrease it below the level of noise, and we have to consider quite large neighbourhoods if we want to obtain unnoisy parameters.

References

[1] A. Dąbrowski, Z. Galias, M.J. Ogorzałek, L.O.Chua, "Laboratory environment for controlling chaotic electronic systems", Proc. European Conference on Circuit Theory and Design, Davos, September 1993.

[2] A. Dąbrowski, Z. Galias, M.J. Ogorzałek, "Strategies for controlling chaos in Chua's circuit", The MTNS'93 International Symposium on the Mathematical Theory of Networks and Systems, Regensburg, 1993.

[3] J. Guckenheimer, P. Holmes, "Nonlinear oscillations, dynamical systems, and bifurcations of vector fields", Springer-Verlag New York, 1983.

[4] M. Komuro, R. Tokunaga, T. Matsumoto, L.O. Chua, A. Hotta, "Global bifurcation analysis of the double scroll circuit", Int. J. of Bifurcation and Chaos, Vol. 1, No. 1 (1991), pp. 139-182.

[5] E. Ott, C. Grebogi, J.A. Yorke "Controlling chaotic dynamical systems", Published in: Chaos – Soviet-American Perspectives on Nonlinear Science, D.K. Campbell ed., American Institute of Physics, New York, 1990, pp.153-172.

[6] T.S. Parker, L.O. Chua, "Practical numerical algorithms for chaotic systems", Springer-Verlag New York, 1989.

[7] F. Zou, J.A. Nossek, Bifurcation and Chaos in Cellular Neural Network, IEEE Trans. on Circuits and Systems, vol. 40, No.3, pp. 166-172, March 1993.